

Targeting 3' and 5' untranslated regions with antisense oligonucleotides to stabilize frataxin mRNA and increase protein expression

Yanjie Li¹, Jixue Li¹, Jun Wang¹, David R. Lynch², Xiulong Shen³, David R. Corey³, Darshan Parekh⁴, Balkrishen Bhat⁴, Caroline Woo⁴, Jonathan J. Cherry⁴, Jill S. Napierala¹ and Marek Napierala^{1,*}

¹Department of Biochemistry and Molecular Genetics, University of Alabama at Birmingham, 1825 University Blvd, Birmingham, AL 35294, USA, ²Division of Neurology and Pediatrics, Children's Hospital of Philadelphia, Abramson Research Center, Room 502, Philadelphia, PA 19104, USA, ³Department of Pharmacology and Biochemistry, University of Texas Southwestern Medical Center, Dallas, TX 75390, USA and ⁴Translate Bio, 29 Hartwell Avenue, Lexington, MA 02421, USA

Received January 20, 2021; Revised September 30, 2021; Editorial Decision October 01, 2021; Accepted October 04, 2021

ABSTRACT

Friedreich's ataxia (FRDA) is a severe multisystem disease caused by transcriptional repression induced by expanded GAA repeats located in intron 1 of the *Frataxin (FXN)* gene encoding frataxin. FRDA results from decreased levels of frataxin; thus, stabilization of the *FXN* mRNA already present in patient cells represents an attractive and unexplored therapeutic avenue. In this work, we pursued a novel approach based on oligonucleotide-mediated targeting of *FXN* mRNA ends to extend its half-life and availability as a template for translation. We demonstrated that oligonucleotides designed to bind to *FXN* 5' or 3' noncoding regions can increase *FXN* mRNA and protein levels. Simultaneous delivery of oligonucleotides targeting both ends increases efficacy of the treatment. The approach was confirmed in several FRDA fibroblast and induced pluripotent stem cell-derived neuronal progenitor lines. RNA sequencing and single-cell expression analyses confirmed oligonucleotide-mediated *FXN* mRNA upregulation. Mechanistically, a significant elongation of the *FXN* mRNA half-life without any changes in chromatin status at the *FXN* gene was observed upon treatment with end-targeting oligonucleotides, indicating that transcript stabilization is responsible for frataxin upregulation. These results identify a novel approach toward upregulation of steady-state mRNA levels via oligonucleotide-mediated end targeting that may be of significance to any condition resulting from transcription downregulation.

INTRODUCTION

Friedreich's ataxia (FRDA) is a severe neurodegenerative disease caused by transcriptional repression induced by expanded GAA repeats located in intron 1 of the *Frataxin (FXN)* gene (1,2). FRDA is the most common inherited ataxia in humans, with ~1 in 100 people carrying a mutation in the *FXN* gene and the overall population frequency reaching 1 in 30 000–50 000 (3,4). There is no effective treatment for FRDA.

The vast majority of FRDA patients are homozygous for large expansions of GAA repeat sequence in intron 1 of the *FXN* gene (5). Repeat expansion leads to deficiency of frataxin, a mitochondrial protein important in biogenesis of iron–sulfur clusters, resulting in widespread metabolic changes in various tissues and organs, including central and peripheral nervous systems, heart and pancreas (4,6,7). FRDA patients always express a detectable level of *FXN*, ranging from ~5% to 35% of levels that can be found across a control cohort (8,9). Importantly, the protein-coding sequence of *FXN* is unaffected in the majority of FRDA patients, indicating that upregulation of endogenous *FXN* levels will be an effective therapy.

Therapeutic avenues currently being explored for FRDA can be classified into two categories: reversing the decreased level of frataxin and alleviating downstream consequences of frataxin deficit (10). Significant efforts have been devoted to reactivate expression of the *FXN* gene by means of reversing chromatin changes associated with GAA expansions (11). Another group of strategies aims to increase levels of frataxin via increasing translation of the existing *FXN* mRNA, direct protein supplementation, *FXN* gene delivery using viral vectors or cell therapy (12–15). Recent, comprehensive reviews describe in detail various therapeutic strategies that are currently being explored for FRDA (11,16).

*To whom correspondence should be addressed. Tel: +1 205 975 5320; Fax: +1 205 975 3335; Email: mnapiera@uab.edu

The currently accepted mechanism of decreased *FXN* gene expression postulates that transcription is reduced (9,11,17). It has been proposed that noncanonical DNA or DNA–RNA structures (R-loops) are responsible for initiation of the transcription defect (18–21). Although it is not clear whether repressive chromatin modifications observed at the *FXN* locus in FRDA cells trigger the silencing or are rather a consequence of the transcriptional downregulation, treatment with histone deacetylase inhibitors and other chromatin targeting molecules stimulates transcription of the *FXN* gene in FRDA cells and animal models (17,22–25).

Recent advances in oligonucleotide (ON) chemistry and breakthrough approvals of critically needed ON-based therapies for neurodegenerative and neuromuscular diseases demonstrated that this approach may also be suitable for targeting frataxin deficiency (26–31). In most cases, ON strategies are intended to silence expression of a target gene or change maturation of pre-mRNA via exon skipping or inclusion (32–34). The concept of ON-mediated activation of gene expression has not been extensively explored; however, it was shown that silencing noncoding transcripts by overlapping a promoter with small RNAs can enhance expression of the target gene (35). Gene activation can also be achieved by correction of splicing and elimination of non-productive alternative splicing products (36). In addition, strategies to increase gene expression by enhancing translation efficiency have also been reported (37,38).

In FRDA, interference with the inhibitory effects of the expanded GAAs was a primary target for ON-mediated intervention in proof-of-concept studies (26–29,39). Initially, it was demonstrated that GAA ONs could alleviate an *in vitro* transcription block and allow for more efficient T7 polymerase transcription through long GAA tracts (31). Also, polyamides specifically binding GAA–TTC tracts prevented formation of triplex-like structures *in vitro* and increased *FXN* transcription in patient lymphoblast cells (18). It has been demonstrated that formation of stable R-loops at expanded GAA tracts may be responsible for inhibiting transcription progression (29). Systematic studies of ONs that target GAA–TTC regions clearly demonstrated that both single-stranded and double-stranded ONs reduce formation of R-loops, reverse chromatin changes and elevate *FXN* transcription in FRDA patient-derived fibroblasts and neuronal progenitor cells (NPCs) (27,28,39). Moreover, gapmers targeting GAA repeats for transcript degradation, likely via targeting *FXN* pre-mRNA engaged in R-loop formation, also augmented levels of *FXN* mRNA and protein (26).

Here, we explore stabilization of *FXN* mRNA as an approach to increase levels of frataxin protein. We hypothesized that ONs targeting the 5' and/or 3' end of the *FXN* mRNA could reduce its susceptibility to degradation, resulting in increased levels of transcript and frataxin protein in FRDA cells. We demonstrate that ONs designed to bind to 5' or 3' untranslated region (UTR) of the *FXN* transcript can increase *FXN* mRNA and protein levels. A combined delivery of ONs targeting both ends increased efficacy of the treatment. Mechanistically, a significant extension of the *FXN* mRNA half-life without FRDA-specific changes

in the chromatin status at the *FXN* locus was observed upon treatment with end-targeting ONs. These results identify a novel approach toward upregulation of steady-state *FXN* mRNA levels via ON-mediated end targeting that may be of significance for any condition resulting from transcription downregulation.

MATERIALS AND METHODS

Cell culture

Human primary fibroblasts were cultured in Dulbecco's modified Eagle medium (DMEM; Thermo Fisher, Cat# 11965092) supplemented with 15% fetal bovine serum (FBS; GE Healthcare Life Sciences, Cat# SH30910.03) and 1% nonessential amino acids (Thermo Fisher, Cat# 11140050) as described earlier (9,40,41). FRDA patient induced pluripotent stem cells (iPSCs) were cultured in mTeSR1™ medium (STEMCELL Technologies, Cat# 05850) as described earlier (42–44). Monolayer NPCs were generated and cultured by using the STEMdiff™ Neural System (STEMCELL Technologies, Cat# 08582, 05833) as described in (27). Briefly, on day 1, the iPSCs were treated with Accutase® (STEMCELL Technologies, Cat# 07920) and plated in wells precoated with Corning™ Matrigel™ hESC-qualified matrix (Thermo Fisher, Cat# 08774552) at a density of 2×10^5 cells/cm² in STEMdiff™ Neural Induction Medium + SMADi + 10 μM Y27632. Media changes were performed daily according to the manufacturer's instructions. The NPCs were ready for the initial passage when cultures reached 90% confluence (typically between days 6 and 9). Cells were plated on Matrigel-coated wells at a density of 2×10^5 cells/cm² and cultured for 5–7 days in STEMdiff™ Neural Induction Medium + SMADi. Subsequently, cells were passaged and cultured in complete STEMdiff™ Neural Progenitor Medium with daily media changes. The NPCs were characterized by immunostaining as described in (27).

ON delivery

ONs targeting *FXN* mRNA ends and control ONs were synthesized by Translate Bio or Qiagen (Table 1). For primary fibroblast lines, Lipofectamine 2000 (Thermo Fisher, Cat# 11668019) was used to deliver ONs. In brief, fibroblasts were seeded into six-well plates at a density of 2×10^5 cells per well the day before transfection. Opti-MEM (Thermo Fisher, Cat# 31985070) was used to prepare Lipofectamine 2000 reagent as well as ONs prior to transfection. For NPCs, the MaxCyte system was used for transfection of ONs using the Optimization 4 electroporation protocol with OC-100 cuvettes (MaxCyte, Inc.), as described in (27). Five hundred thousand cells in a volume of 50 μl were added to an OC-100 cuvette and electroporation was performed. Immediately after transfection, 50 μl of warm maintenance medium was added to the cuvettes, and the cuvettes were closed and rested in an incubator (37°C and 5% CO₂) for 15 min. Cells were then plated onto 12-well plates precoated with Matrigel. Frataxin expression was assayed by qRT-PCR after 72 h.

Table 1. Targeting sequences and modifications of ONs used for these studies

Oligo	Target	Type	Target sequence (5'→3')	Modification
<i>FXN mRNA targeting</i>				
ET2 ^a	<i>FXN</i> 5' UTR	Mixmer	CGCTCCGCCCTCCAG	InaCs;InaGs;InamCs;dTs;InamCs;dCs;InaGs;dCs;InamCs;dCs;InaTs;omeCs;InamCs;InaAs;InaG
ET14 ^a	<i>FXN</i> 5' UTR	Mixmer	CCGGGTCTGCCGCC	omeCs;InamCs;dGs;InaGs;dGs;InaTs;dCs;InaTs;dGs;InamCs;dCs;InaGs;dCs;InamCs;omeC
ET0	<i>FXN</i> 5' UTR	Mixmer	TGACCAAGGGAGAC	dTs;InaGs;dAs;InamCs;dCs;InamCs;dAs;InaAs;dGs;InaGs;dGs;InaAs;dGs;InaAs;dC
ET5	<i>FXN</i> 5' UTR	Mixmer	TGGCCACTGGCCGCA	dTs;InaGs;dGs;InamCs;dCs;InaAs;dCs;InaTs;dGs;InaGs;dCs;InamCs;dGs;InamCs;dA
ET9	<i>FXN</i> 5' UTR	Mixmer	CGGCGACCCCTGGTG	dCs;InaGs;dGs;InamCs;dGs;InaAs;dCs;InamCs;dCs;InamCs;dTs;InaGs;dGs;InaTs;dG
ET10	<i>FXN</i> 5' UTR	Mixmer	CGCCCTCCAGCGCTG	dCs;InaGs;dCs;InamCs;dCs;InaTs;dCs;InamCs;dAs;InaGs;dCs;InaGs;dCs;InaTs;dG
EX50	<i>FXN</i> exon	Mixmer	CGGCGCCGAGAGTCCACAT	dCs;InaGs;dGs;InamCs;dGs;InamCs;dCs;InamCs;dGs;InaAs;dGs;InaAs;dGs;InaTs;dCs
EX52	<i>FXN</i> exon	Mixmer	CCAGGAGGCCGGCTACTGCG	;InamCs;dAs;InamCs;dAs;InaT
EX60	<i>FXN</i> exon	Mixmer	CTGGGCTGGGCTGGGTGACG	dCs;InamCs;dAs;InaGs;dGs;InaAs;dGs;InaGs;dCs;InamCs;dGs;InaGs;dCs;InaTs;dAs;In
EX70	<i>FXN</i> exon	Mixmer	TCAAGCATCTTTCCGGAA	amCs;dTs;InaGs;dCs;InaG
ET3 ^a	<i>FXN</i> 3' UTR	Mixmer	ATUAUTUTGCUTUTT	dCs;InaTs;dGs;InaGs;dGs;InamCs;dTs;InaGs;dGs;InaGs;dCs;InaTs;dGs;InaGs;dGs;Ina
ET4 ^a	<i>FXN</i> 3' UTR	Mixmer	CCTCAAAGCAGGAAUA	Ts;dGs;InaAs;dCs;InaG
ET7	<i>FXN</i> 3' UTR	Mixmer	TCCTTAAACGGGGCTGGGCA	dTs;InamCs;dAs;InaAs;dGs;InamCs;dAs;InaTs;dCs;InaTs;dTs;InaTs;dTs;InamCs;dCs;l
ET12	<i>FXN</i> 3' UTR	Mixmer	CATAATGAAGCTGGG	naGs;dGs;InaAs;dA
ET21	<i>FXN</i> 3' UTR	Mixmer	AACAACAACAACAACAAAAAC	InaAs;InaTs;fluUs;InaAs;fluUs;InaTs;fluUs;InaTs;fluUs;InaTs;InaT
ET24	<i>FXN</i> 3' UTR	Mixmer	GCTGTGACACATAGCCCAACTG	InamCs;omeCs;InaTs;omeCs;InaAs;omeAs;InaAs;omeAs;InaGs;omeCs;InaAs;omeGs;l
ET18	<i>FXN</i> 3' UTR	Mixmer	AGGAGGCAACACATT	naAs;omeAs;InaAs;omeUs;InaA
ET25	<i>FXN</i> 3' UTR	Mixmer	GTAGGCTACCCTTTA	dTs;InamCs;dCs;InaTs;InaAs;dAs;InaAs;dAs;InamCs;dGs;InaGs;dGs;InaGs;dCs;In
ET17	<i>FXN</i> 3' UTR	Mixmer	GGGGTCTGGCCTGA	dAs;InaAs;dCs;InaAs;dAs;InamCs;dAs;InaCs;InaAs;dAs;InamCs;dAs;InaAs;dCs;In
ET6	<i>FXN</i> 3' UTR	Mixmer	CATTTTCCCTCCTGG	aAs;InamCs;dAs;InaGs;dTs;InaGs;dAs;InamCs;dAs;InaTs;dAs;InaGs;dCs;l
<i>Control</i>				
Gap	<i>FXN</i> mRNA	Gapmer	GGCATAAGACATTAT	namCs;dCs;InaAs;dAs;InamCs;dTs;InaGs;dT
CM	Nontarget	Mixmer	GCTATACCAGCGTCGCAT	dAs;InaGs;dGs;InaAs;dGs;InaGs;dCs;InaAs;dAs;InamCs;dAs;InaCs;InaAs;dAs;InaT
RN-0012	Nontarget	Mixmer	AGAUGCAGTGUCUCUT	dGs;dCs;InaTs;dAs;dTs;InaAs;dCs;dCs;InaAs;dGs;dCs;InaGs;dTs;dCs;InaGs;dTs;dCs;
siRNA-1 ^b	GAA positive control	siRNA	TUCUUCUUCUUCUUCUUA	InaAs;dT
BNA-2 ^b	GAA positive control	BNA	TTCTTCTTCTTCT	InaAs;omeGs;InaAs;omeUs;InaGs;omeCs;InaAs;omeGs;InaTs;omeGs;InamCs;omeUs;l
				namCs;omeUs;InaT
				InaTs;omeUs;InamCs;omeUs;omeUs;InamCs;omeUs;omeUs;InamCs;omeUs;omeUs;l
				namCs;omeUs;omeUs;InamCs;omeUs;omeUs;InamCs;omeUs;InaAs;InaA
				InaTs;InaTs;InamCs;InaTs;dTs;dCs;dTs;dTs;dCs;dTs;dTs;dCs;dTs;InaTs;InamCs;InaT

Deoxyribonucleic acid, locked nucleic acid, 2'-O-methyl and 2'-fluoro-modified nucleotides were used for the synthesis of the end targeting and control ONs. dN, deoxynucleotide; s, phosphorothioate; ome, 2'-O-methyl; Ina, locked nucleic acid; flu, 2'-fluoro; and mC, methylcytosine. The mixmers were designed to have the listed modifications interspersed throughout the length of the oligos.

^aONs that induced statistically significant increase of *FXN* mRNA level.

^bFor details, see (29,39).

RNA isolation and quantitative real-time RT-PCR

Total RNA was extracted using the RNeasy Mini Kit (Qiagen, Cat# 10074) and treated with DNase I (TURBO DNA-free; Thermo Fisher, Cat# AM1907) for 1 h according to the manufacturer's protocol. The qRT-PCR reactions were assembled using the Power SYBR Green RNA-to-CT 1-Step Kit (Thermo Fisher, Cat# 4391178) and run on a Step-One Plus System (Applied Biosystems) as we described in (41,45). Reverse transcription was conducted at 48°C for 30 min, followed by 40 cycles of denaturation at 95°C for 15 s, annealing at 55°C for 20 s and elongation for 1 min at 60°C. All reactions were performed in triplicate. Control reactions were also performed without reverse transcriptase to confirm removal of genomic DNA. All primers used for qRT-PCR analyses are listed in Supplementary Table S1.

Microfluidic single-cell real-time quantitative PCR

Fibroblasts were detached from the cell culture plates using trypsin as described earlier and resuspended in ice-cold phosphate-buffered saline. Single-cell analyses were performed using the Fluidigm C1 system in combination with standard qPCR method. In brief, 17–25- μ m

Fluidigm integrated fluidic circuits (Fluidigm, Cat# 100-5758) and C1 Single-Cell Auto Prep Reagent Kit (Fluidigm, Cat# 100-5319) were used to capture and lyse individual cells. Subsequently, reverse transcription and pre-amplification were performed using PreAmp Ambion Single Cell-to-CT™ qRT-PCR Kit (Life Technologies, Cat# 4458237). The pre-amplified products served as templates for qPCR to determine *FXN* mRNA level using a Viia 7 Real-Time PCR System (Invitrogen). Reactions were carried out by 40 cycles of denaturation at 95°C for 15 s, annealing at 55°C for 20 s and elongation for 1 min at 60°C. The Power SYBR™ Green PCR Master Mix Kit (Thermo Fisher, Cat# 4367659) was used for all single-cell qPCR reactions.

RNA sequencing

A total of 1 μ g RNA was used for each RNA sequencing (RNA-seq) reaction. A second DNase I treatment was performed for all samples to eliminate genomic DNA contamination. RNA-seq was conducted using polyA-enriched RNAs. Sequencing libraries were prepared using TruSeq Kit (Illumina, San Diego, CA) and sequenced on an Illumina 2500 Genetic Analyzer at the UAB Hefflin Center

for Genomic Sciences. Seventy-five base pair reads were mapped using STAR aligner (v2.6.1d) to hg38 (RefSeq Transcripts 88, 1 February 2019). Quantitative analysis of gene expression was conducted using DESeq2 (v3.5). Details regarding number of reads per sample and sequencing quality are presented in Supplementary Table S2. Normalized reads mapped to the *FXN* locus were visualized using PartekFlow (Partek, St Louis, MO).

Quantitative measurement of *FXN* mRNA stability

The *FXN* mRNA stability was analyzed by a pulse-chase method using the Click-IT[®] Nascent RNA Capture Kit (Thermo Fisher, Cat# C10365). For each experiment, five six-well plates of fibroblasts were plated at a density of 2×10^5 cells per well. Twenty-four hours after plating, half of the wells (15 wells) were treated with ET(14 + 4) (30 nM each), while the remaining wells were treated by vehicle only (Lipofectamine 2000). After 24 h, all cells were pulsed with 0.2 mM ethylene uridine (EU) and cultured for an additional 12 h. Next, cells were washed three times with Dulbecco's phosphate-buffered saline, and EU-containing medium was replaced with a standard DMEM/15% FBS medium. Cells were collected at five time points for analysis: 0, 6, 12, 24 and 48 h. Three wells of cells were harvested per each time point. Total RNA was isolated from cells using TRIzol Reagent (Invitrogen, Cat# 1596026). To ensure adequate normalization of the final qRT-PCR step and appropriate calculation of *FXN* mRNA half-life, an exogenous GFP RNA spike-in control was included in subsequent purification steps. The GFP RNA was *in vitro* synthesized by T7 RNA polymerase in the presence of 10 mM EU. A HiScribe[™] T7 ARCA mRNA Kit (New England Biolabs, Cat# E2065S) was used for *in vitro* transcription, and the pCAG-FLPe-GFP plasmid (Addgene #13788) was used as a template. The EU-labeled RNA samples were then subjected to biotinylation via a click reaction, followed by binding to Streptavidin T1 magnetic beads, washing and reverse transcription according to the manufacturer's recommendations. The obtained cDNA was used in qPCR reactions to quantify the EU-labeled transcripts: *FXN*, *ACT1* and *NEAT1*. Sequences of primers used are listed in Supplementary Table S1.

To define the half-life of each RNA, the expression level was calculated using $\Delta\Delta\text{Ct}$ method with normalization to the spiked-in GFP RNA. The exponential decay constants (λ) were solved by nonlinear regression of the percentage of the remaining RNA versus time. RNA half-lives were calculated using the equation $t_{1/2} = \ln(2)/\lambda$, in which λ is the decay constant as described in (46).

Protein isolation and quantitation

Cells were trypsinized or treated with Accutase[®] and collected by centrifugation at $200 \times g$ for 5 min. Cell lysates were prepared using Passive Lysis Buffer (Promega, Cat# E1941) supplemented with protease inhibitor cocktail (Sigma-Aldrich, Cat# P8340). After three freeze-thaw cycles, the lysates were centrifuged at $13\,000 \times g$ for 15 min at 4°C. Protein concentration was determined using Bradford Protein Assay Kit (Bio-Rad, Cat# 500-

0006). Twenty micrograms of whole cell extract was electrophoresed on NuPAGE 4–12% Bis-Tris gels (Life Technologies, Cat# NP0321BOX) followed by transfer onto 0.2- μm nitrocellulose membrane (Bio-Rad, Cat# 165-0112). Membranes were then stained with Ponceau S and documented using a ChemiDoc MP Imaging System (Bio-Rad). Frataxin was detected using anti-FXN at 1:1000 (Santa Cruz, Cat# SC-25820) for 12 h at 4°C. Actin was detected using anti-ACTIN monoclonal antibody (Santa Cruz, Cat# SC-47778) at 1:2000 for 12 h at 4°C. Horseradish peroxidase-conjugated rabbit anti-mouse immunoglobulin (GE Healthcare Life Sciences, Cat# NA934V) and donkey anti-rabbit immunoglobulin (GE Healthcare Life Sciences, Cat# NA931V) were used as secondary antibodies and incubated for 1 h at room temperature at 1:5000. Signal was quantified by using Image Lab 6.0.1 software (Bio-Rad).

Chromatin immunoprecipitation

Chromatin immunoprecipitation (ChIP) was performed as described in (9). Immunoprecipitated chromatin was purified using phenol/chloroform extraction and ethanol precipitation before qPCR. The qPCR was conducted using the Power SYBR Green-CT Kit (Step-One Plus System, Applied Biosystems). Thermal cycling was carried out as follows: 10 min at 94°C, 40 cycles of 30 s at 94°C followed by 60 s at 60°C. Sequences of the primers are listed in Supplementary Table S1. The relative abundance of histone H3K9ac and H3K9me3 was determined by normalizing the quantities of the immunoprecipitated sample to the quantity of total histone H3 after normalization to input reactions (% input).

Statistical analyses

All statistical analyses, except for RNA-seq, were conducted using GraphPad Prism 6 software. Statistical significance was determined by Student's *t*-test or ANOVA and $P < 0.05$ was considered significant. For RNA-seq, statistical analyses of the data were conducted using the default settings on the DESeq2 package version 3.5. In figures, '*n*' designates the number of biological replicates.

RESULTS

Identification of *FXN* activating ONs

To identify ONs that target the *FXN* mRNA and increase its level in FRDA cells, we screened a library of 20 mixmer ONs (Table 1) targeting predominantly 5' and 3' UTRs of the transcript. As a control, the library included a gapmer targeting *FXN* mRNA 3' UTR designed to decrease levels of the *FXN* transcript. The ONs were transfected in triplicate to FRDA fibroblast line F1 (Figure 1A). These cells contain two expanded GAA tracts of 400 and 470 repeats and express a low level of the *FXN* mRNA (Figure 1A). Quantitative qRT-PCR analyses demonstrated variable effect of ONs on *FXN* mRNA levels and identified four end-targeting ONs, ET2, ET14, ET3 and ET4, capable of increasing *FXN* transcript by >1.5-fold ($P < 0.05$) compared to vehicle control (Figure 1B).

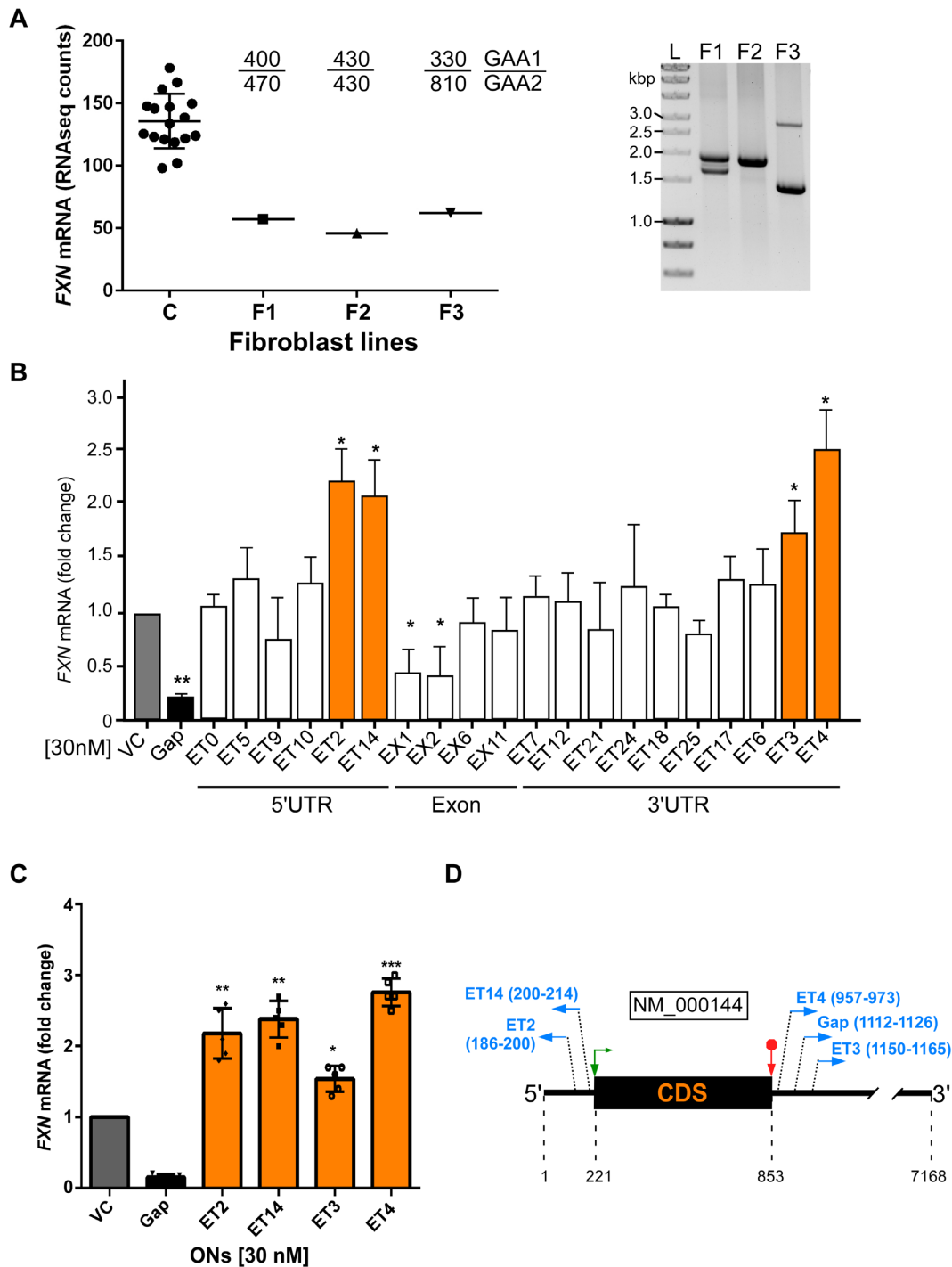


Figure 1. End-targeting ONs increase the level of *FXN* mRNA in FRDA fibroblasts. (A) Reduced expression of *FXN* mRNA in selected FRDA fibroblast lines (F1–F3) compared to a cohort of unaffected controls. Data from RNA-seq analyses are presented (GSE104288). The number of GAA repeats determined for GAA1 and GAA2 alleles is indicated. On the right, agarose gel analysis of long GAA PCR products to determine number of repeats in each cell line; L indicates 1 kb plus DNA ladder. (B) Results of the qRT-PCR screen to identify ONs capable of increasing *FXN* mRNA levels. Detailed information regarding ONs used in the screen is presented in Table 1. The screen was conducted in triplicate in F1 fibroblasts ($n = 3$). Asterisks indicate $*P < 0.05$. (C) qRT-PCR analysis of *FXN* mRNA levels in FRDA fibroblasts transfected with individual end-targeting ONs (orange bars) relative to vehicle control (VC, gray bar). A gapmer (Gap, black bar) targeting the *FXN* mRNA was used as a positive control for transfection. All ONs were transfected using Lipofectamine 2000 at 30 nM final concentration. Results are an average of at least five experiments ($n > 5$) performed in three fibroblast lines. Error bars indicate standard deviation (StDev); $*P < 0.05$. (D) Schematic presentation of the *FXN* mRNA (NM_000144; not to scale). Location and nucleotide position of translation start codon (green arrow), stop codon (red symbol) and coding sequence (CDS; black bar) are shown. Exact positions of the end-targeting ONs (ET2, ET3, ET4 and ET14) and control gapmer (Gap) are indicated.

To confirm the effect of these four ONs on *FXN* mRNA, we transfected ET2 and ET14 targeting the 5' end and ET3 and ET4 targeting the 3' end of the *FXN* mRNA (Table 1) into three different FRDA lines (F1, F2 and F3; Figure 1A and C). All ONs elevated levels of frataxin mRNA by 1.5–2.5-fold in FRDA cells when compared to control (Figure 1C). Both 5' UTR ONs recognize sequences in proximity of the ATG codon, while the 3' ONs mapped within 300 bp of the stop codon and surround major polyadenylation sites identified in the *FXN* mRNA (Figure 1D). Although the NCBI database of reference sequences indicates that the *FXN* mRNA contains 220 bases of transcript prior to the ATG start codon (NM_000144), detailed analyses of *FXN* transcripts using the University of California, Santa Cruz Genome Browser and our deep RNA-seq dataset [conducted on 18 FRDA and 17 control fibroblast lines (9)] demonstrate that the noncoding 5' end of the *FXN* transcript is shorter and likely does not exceed 68 nucleotides (Supplementary Figure S1).

Simultaneous targeting of 5' and 3' ends potentiates effect of individual ONs on *FXN* mRNA

After demonstrating that the administration of single ONs increased levels of *FXN* mRNA, we hypothesized that simultaneously targeting the 5' and 3' ends would achieve higher levels of *FXN* transcript. All four combinations of the initially identified end-targeting ONs were transfected to FRDA fibroblasts at a concentration of 30 nM each. Indeed, the level of *FXN* mRNA detected via qRT-PCR increased to ~4–5-fold over control upon simultaneous targeting of both mRNA ends (Figure 2A).

To minimize potential qRT-PCR bias that may be caused by changes in expression of selected housekeeping genes upon ON treatment (47), in addition to standard normalization (*GAPDH* mRNA level), we utilized total RNA levels to normalize *FXN* mRNA signal. The results are presented as a change in absolute Ct value detected for the *FXN* transcript with all qRT-PCR analyses performed using 50 ng of total RNA (Figure 2B). A significant decrease of the Ct value (increase of expression) was observed for all four ON pairs. We found this method to be a very reliable indicator of actual changes in *FXN* mRNA levels.

FXN increase is also detected in NPCs

Although primary fibroblasts have been widely used for studying transcription of the *FXN* gene (9,29,39,41,48), it is essential to also determine the efficacy of ON treatment in human cells relevant to disease pathology. We tested ON pairs using FRDA NPCs differentiated from iPSCs. In agreement with the fibroblast data, we observed a significant, 2–3-fold increase of *FXN* mRNA levels relative to controls (Figure 2C). It is important to note that NPCs require electroporation-mediated delivery of the ONs at higher concentrations (5 μ M each) than fibroblasts. Using FRDA NPCs, we also compared efficacy of end-targeting ONs to ONs known to increase *FXN* expression via targeting the GAA repeats [siRNA-1 and BNA-2 (39); Table 1]. Analyses demonstrated similar upregulation of *FXN* mRNA using both approaches (Figure 2C).

FXN mRNA increase is reflected in upregulation of frataxin level in FRDA cells

To evaluate whether changes in transcript abundance caused by ON treatment translate into elevated frataxin protein levels, we performed western blot analyses. Depending on the ON pair, an average of 1.5–2-fold higher levels of frataxin protein were detected in treated cells relative to vehicle control cells after normalization to total protein expression (Ponceau S) (Figure 2D and E). These results indicate that the ON-mediated mRNA increase is reflected, albeit to a lesser magnitude, in overall higher frataxin protein levels. To define a possible cause of the quantitative discrepancy between *FXN* transcript and protein increase, we tested the effect of individual ONs in comparison to the combination of ONs on frataxin levels. Experiments were conducted in three different FRDA fibroblast lines with the most efficacious set of ONs: ET4, ET14 and ET(14 + 4). Results of these analyses showed that efficacy of individual ONs was similar to ET(14 + 4) combined (Figure 2F and G), suggesting that combining the ONs may affect efficiency of translation to a greater extent than individual ONs.

ON treatment increases *FXN* mRNA but not protein levels in control cells

Results of the studies using four pairs of end-targeting ONs showed that the ET(14 + 4) pair demonstrated the greatest potency and reproducibility (Figure 2A–E). Therefore, we focused our further analyses of the mechanism of *FXN* transcript upregulation on this pair. To determine whether these ONs can upregulate levels of *FXN* mRNA and protein in control cells, we treated two control lines with 30 nM ET4, ET14 and ET(14 + 4). Quantitative RT-PCR demonstrated a strong upregulation of the *FXN* transcript, especially by simultaneous treatment with ET(14 + 4) (Figure 3A). However, western blot analyses showed no increase of frataxin protein levels in control cells (Figure 3B and C). These results, although surprising, are not completely unexpected. Recent studies demonstrate that overexpression of frataxin may be as toxic as its depletion (49,50). Thus, it is possible that intracellular mechanisms exist preventing high expression of endogenous frataxin beyond a tolerable threshold.

Activation is sequence selective

The difference in *FXN* gene expression between full expression in control cells and reduced expression in FRDA cells is only ~3-fold (Figure 1A). This relatively small change makes it essential to establish that activation is not an off-target effect or artifact. We tested several ONs of similar composition but lacking sequence complementarity to the *FXN* transcript. These compounds did not result in increased *FXN* at either the mRNA or protein level (Figure 4A and B), authenticating the effects of the *FXN* end-targeting ONs.

As one potential off-target effect of nucleic acid treatment is stimulation of the interferon response (29), we tested expression of *IFITM1*, *IRF9*, *MX1*, *OAS1* and *OAS2* genes

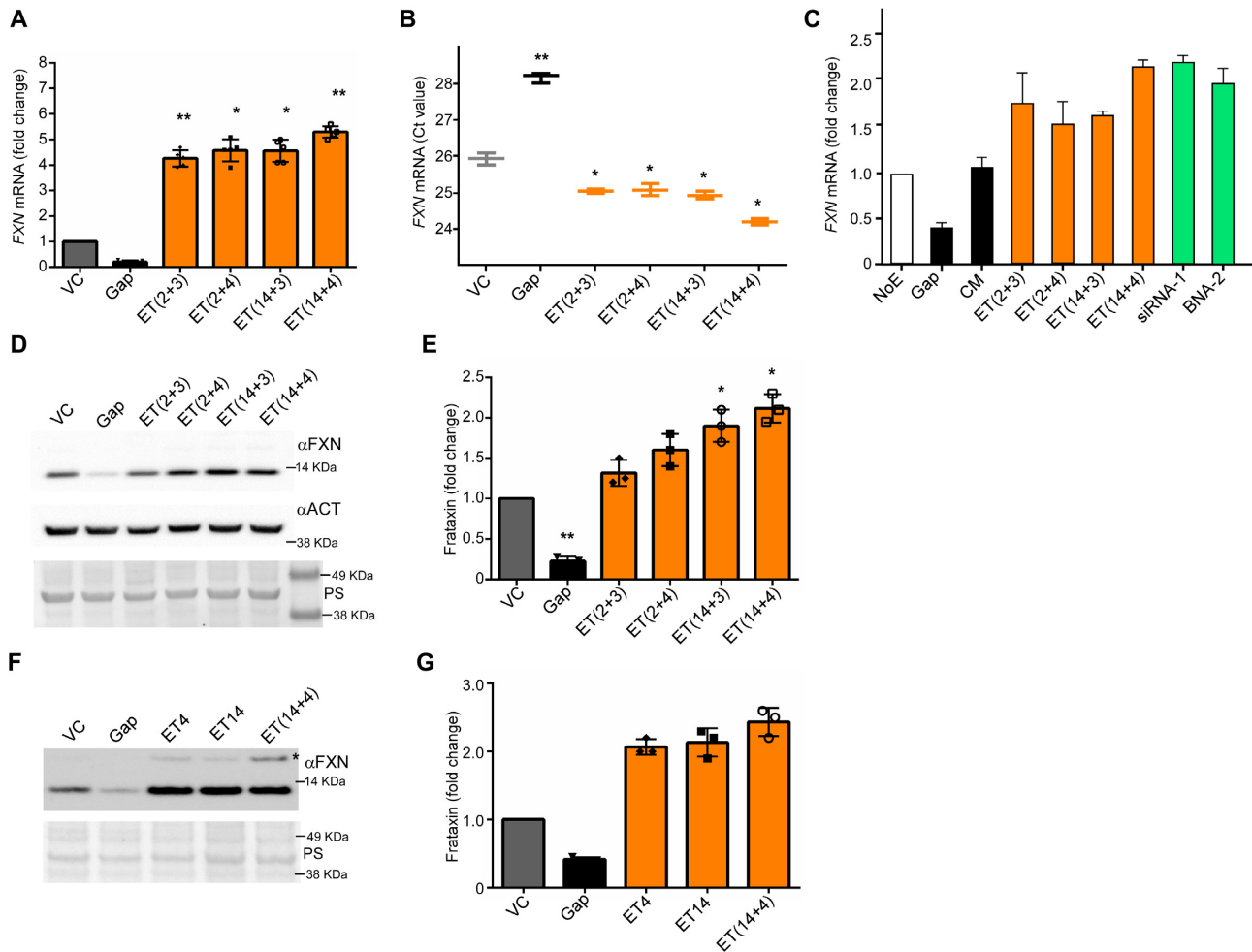


Figure 2. Simultaneous targeting of 5' and 3' *FXN* mRNA ends increases level of frataxin. (A) qRT-PCR analysis of the *FXN* mRNA level in FRDA fibroblasts transfected with pairs of end-targeting ONs (orange bars; ONs included in a pair are indicated in parentheses) relative to vehicle control (VC, gray bar). A gapper (Gap, black bar) targeting the *FXN* mRNA was used as a positive control for transfection. All ONs were transfected using Lipofectamine 2000 at 30 nM each (60 nM combined final concentration). Results are an average of at least five experiments ($n > 5$). Error bars indicate StDev; * $P < 0.05$, ** $P < 0.01$. (B) Normalizer-independent analysis of *FXN* mRNA levels in FRDA fibroblasts using qRT-PCR. Expression of the transcript is normalized to the total RNA used in each reaction (identical for all samples) and expressed as Ct values. Lower Ct value indicates higher *FXN* mRNA level. Results of a representative experiment are shown as average of three technical PCR replicates. Error bars indicate range. (C) End-targeting ONs increase *FXN* mRNA levels in FRDA NPCs. The iPSC-derived NPCs were electroporated with end-targeting ONs (at 5 μ M each, orange bars). Nonelectroporated cells (NoE, white bar) were used as the control to calculate fold change of *FXN* transcript level. Five micromolar gapper (Gap, black bar) was used as a positive control for transfections. Nontargeting ON (CM at 5 μ M, black bar) was used for comparison to NoE cells. For comparison, cells were transfected in parallel with 5 μ M siRNA-1 or 5 μ M BNA-2 ONs (green bars) shown in previous studies to reactivate *FXN* mRNA expression by direct targeting of the expanded GAA tract (29,39). Data were collected from two independent experiments ($n = 2$). (D) Western blot analysis of frataxin expression in FRDA fibroblasts transfected with end-targeting ON pairs (ONs included in a pair are indicated in parentheses). Equal amounts of protein extract were loaded onto the gel and blotted with frataxin (α FXN)- and actin (α ACT)-specific antibodies; Ponceau S staining (PS) as a control for total protein loading is shown. (E) Quantification of frataxin protein level in FRDA fibroblasts transfected with ON pairs. Data were normalized to Ponceau S. Results are an average of at least three independent transfection experiments ($n > 3$). Error bars indicate StDev; * $P < 0.05$, ** $P < 0.01$. (F) Western blot analysis of frataxin expression in FRDA fibroblasts transfected with individual ET4 and ET14 ONs and ET(14 + 4) pair. Equal amounts of protein extract were loaded onto the gel and blotted with frataxin (α FXN); Ponceau S staining (PS) as a control for total protein loading is shown. Asterisk designates intermediate form of frataxin (before final maturation step). (G) Quantification of frataxin protein level in FRDA fibroblasts transfected with indicated ONs. Image Lab software (Bio-Rad) was used to quantify frataxin signal relative to vehicle control (VC). Data were normalized to Ponceau S. Results are an average of at least three independent transfection experiments ($n > 3$). Error bars indicate StDev; * $P < 0.05$, ** $P < 0.01$.

upon treatment with ET(14 + 4), nontargeting ON and vehicle control. No activation of this panel of interferon responsive genes by ET(14 + 4) was detected (Figure 4C).

ON treatment increases *FXN* mRNA above the control level

Next, we confirmed activity of the ET(14 + 4) in several primary fibroblast lines established from different FRDA

patients (Figure 5A). Furthermore, to verify ET(14 + 4) efficacy toward increasing *FXN* mRNA levels using unbiased approaches, we conducted RNA-seq analyses of RNA isolated from FRDA cells treated with this ON pair or vehicle-treated, as well as control, non-FRDA cells (Figure 5B and C). Results of two independent experiments demonstrated a significant ($P < 0.0003$), ~3-fold increase of

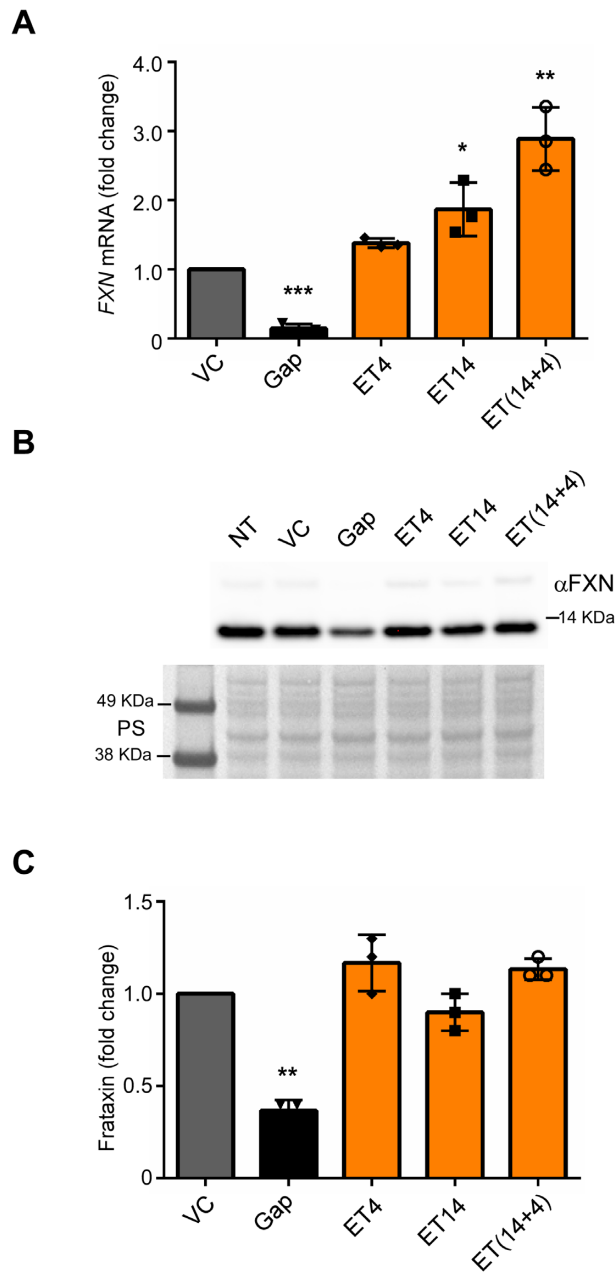


Figure 3. Targeting control cells increases FXN mRNA but not protein levels. (A) qRT-PCR analysis of the *FXN* mRNA level in control fibroblasts transfected with end-targeting ONs (orange bars; ONs included in a pair are indicated in parentheses) relative to vehicle control (VC, gray bar). A gapmer (Gap, black bar) targeting the *FXN* mRNA was used as a positive control for transfection. Individual ONs were transfected at 30 nM each [30 nM each for ET(14 + 4)]. Results are an average of three experiments ($n = 3$) in three different control lines. Error bars indicate StDev; * $P < 0.05$, ** $P < 0.01$. (B) Representative western blot analysis of frataxin expression in control fibroblasts transfected with indicated ONs. Equal amounts of protein extract were loaded onto the gel and blotted with frataxin (α FXN); Ponceau S staining (PS) as a control for total protein loading is shown. NT designates nontransfected control cells. (C) Quantification of frataxin protein level in control fibroblasts transfected with indicated ONs. Image Lab software (Bio-Rad) was used to quantify frataxin signal relative to vehicle control (VC). Data were normalized to Ponceau S. Results are an average of three independent experiments ($n = 3$) in three different control lines. Error bars indicate StDev; ** $P < 0.01$.

FXN mRNA levels in FRDA cells treated with ET(14 + 4) pair compared to the vehicle-treated FRDA cells. Moreover, a comparison between ET(14 + 4)-treated FRDA fibroblasts and two control, non-FRDA fibroblast lines revealed that ON treatment increased *FXN* transcript to levels detected in unaffected cells (Figure 5C). In addition to the observed *FXN* mRNA increase, global transcriptome analysis demonstrated that treatment with ET(14 + 4) corrected expression of ~900 transcripts differentially expressed in FRDA cells to levels comparable to control cells (Supplementary Figure S3). We also utilized this RNA-seq dataset in combination with *in silico* analyses to evaluate potential off-target effects of the treatment (Supplementary Table S3).

Lastly, we quantified *FXN* transcripts at the single-cell level. The ET(14 + 4)-treated and vehicle control FRDA cell populations were analyzed as single cells using the Fluidigm C1 platform. qRT-PCR analyses of *FXN* expression in 66 individual ET(14 + 4)-treated cells and 88 control single cells revealed an average of ~2.1 Ct (normalized to a single cell) difference between these groups, indicating significant ($P = 0.0002$) upregulation of the *FXN* transcript in individual cells following ON treatment (Figure 5D). Parallel standard qRT-PCR analysis of the bulk population of cells used for the single-cell experiment revealed a very similar level of *FXN* increase (Figure 5E).

FXN increase is dose dependent

Next, to determine efficacy of the ET(14 + 4) pair, we performed analyses of *FXN* mRNA expression as a function of ON concentration (Figure 6). Increasing the amount of ET(14 + 4) from 5 to 40 nM resulted in corresponding accumulation of the *FXN* mRNA, with the calculated EC_{50} ranging from 11.3 to 17.5 nM (Figure 6A). Concentration-dependent accumulation of frataxin protein was also observed; however, the level of increase was ~2.5-fold lower (at 30 nM) than that for the *FXN* transcript (Figure 6B).

ON treatment does not affect histone modification

Increased transcription of the *FXN* gene after treatment of FRDA cells with GAA repeat-specific ONs or compounds that target chromatin-modifying enzymes is accompanied by changes of histone modifications near the expanded GAA repeats (29). Upon induction of transcription in FRDA cells, heterochromatin-like histone modifications, including H3K9me3, were decreased and active chromatin marks (e.g. H3K9ac) became overrepresented when compared to nontreated cells. Thus, the chromatin environment of FRDA cells treated with these compounds resembled control, unaffected cells lacking expanded GAA repeats. We conducted ChIP analyses of the *FXN* gene in the vicinity of the expanded GAAs in FRDA cells treated with ET(14 + 4) or vehicle control using antibodies specific for histone H3K9me3 and H3K9ac, i.e. histone modifications most frequently reported to discriminate FRDA and control cells (9,23,51). Importantly, we observed no statistical difference in representation of these marks upon treatment with ONs compared to vehicle-treated controls, thus indicating that the increased level of *FXN* mRNA is not caused

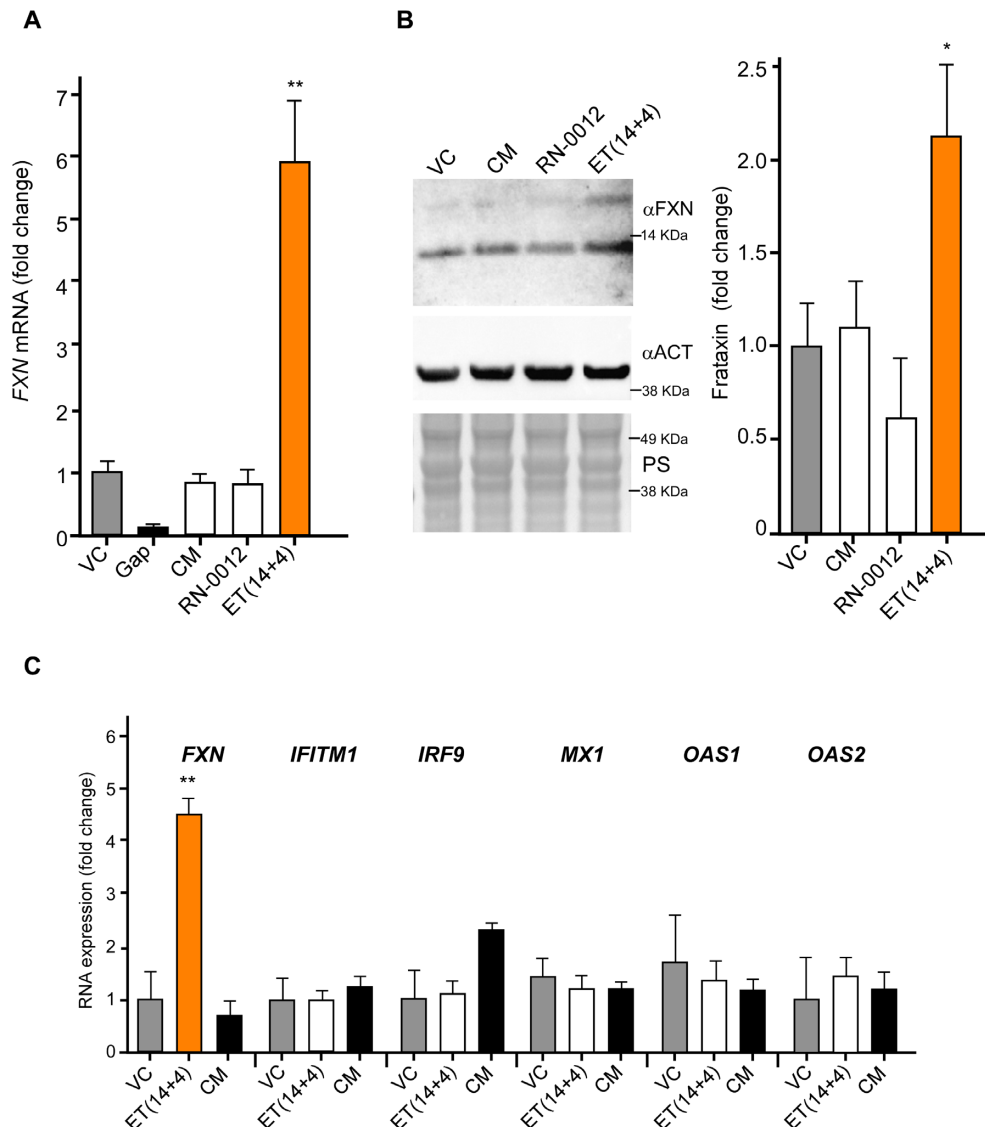


Figure 4. Effect of nontargeting control ONs on frataxin levels. Effect of nontargeting ONs, CM and RN-0012, on *FXN* mRNA (A) and protein (B). Vehicle control (VC, gray bar) and control ONs (CM and RN-0012, each transfected at 60 nM; white bars) did not increase *FXN* transcript or protein levels. Gapmer (Gap, black bar) is shown as a positive control. FRDA fibroblasts were transfected with 60 nM ONs [for ET(14 + 4) pair, 30 nM each]. Data for *FXN* mRNA were collected from at least three independent experiments ($n > 3$) and for frataxin protein from two independent experiments ($n = 2$). Error bars indicate StDev; * $P < 0.05$, ** $P < 0.01$. (C) ET(14 + 4) does not induce expression of interferon responsive genes. qRT-PCR data demonstrate no significant effect of ET(14 + 4) transfection compared with vehicle and ON controls (VC, gray bars; CM, black bars) on the mRNA expression of interferon responsive genes in FRDA fibroblasts. Cells were transfected with 30 nM ONs and RNA isolated 48 h post-transfection. Levels of *FXN* mRNA were also determined as a positive control. Data represent an average of three independent experiments ($n = 3$). Error bars indicate StDev; ** $P < 0.01$. *GAPDH* mRNA was used as a normalizer. The interferon responsive genes tested were interferon induced transmembrane protein 1 (IFITM1), interferon regulatory factor 9 (IRF9), MX dynamin like GTPase 1 (MX1), 2'-5'-oligoadenylate synthetase 1 (OAS1) and 2'-5'-oligoadenylate synthetase 2 (OAS2).

by reversal of chromatin changes near the expanded GAAs (Figure 7A). This result indicates that the end-targeting ONs primarily affect post-transcriptional steps of gene expression, such as mRNA turnover/stability.

End-targeting ONs increase *FXN* mRNA half-life

To determine *FXN* mRNA half-life ($t_{1/2}$) upon ET(14 + 4) treatment, we employed metabolic labeling with 5-ethynyl uridine (Figure 7B) (52,53). Prior analyses demonstrated that *FXN* mRNA $t_{1/2}$ is ~6 h in human lymphoblasts (54); therefore, global transcription inhibitors could not be uti-

lized. Results of three independent experiments showed that ET(14 + 4) increased *FXN* mRNA $t_{1/2}$ from ~5 h in untreated cells to ~14 h ($P < 0.009$) (Figure 7C). At the same time, no significant changes were detected in $t_{1/2}$ of *ACT1* mRNA (~13.5 h) and *NEAT1* noncoding RNA (~5 h) (Figure 7C and Supplementary Figure S4). A GFP spike-in control RNA was used for normalization of the qRT-PCR signals (see the 'Materials and Methods' section). Similar results were obtained in control cells where ET(14 + 4) extended *FXN* mRNA $t_{1/2}$ by ~4.5 h without affecting *ACT1* mRNA (Supplementary Figure S5). Interestingly, we also

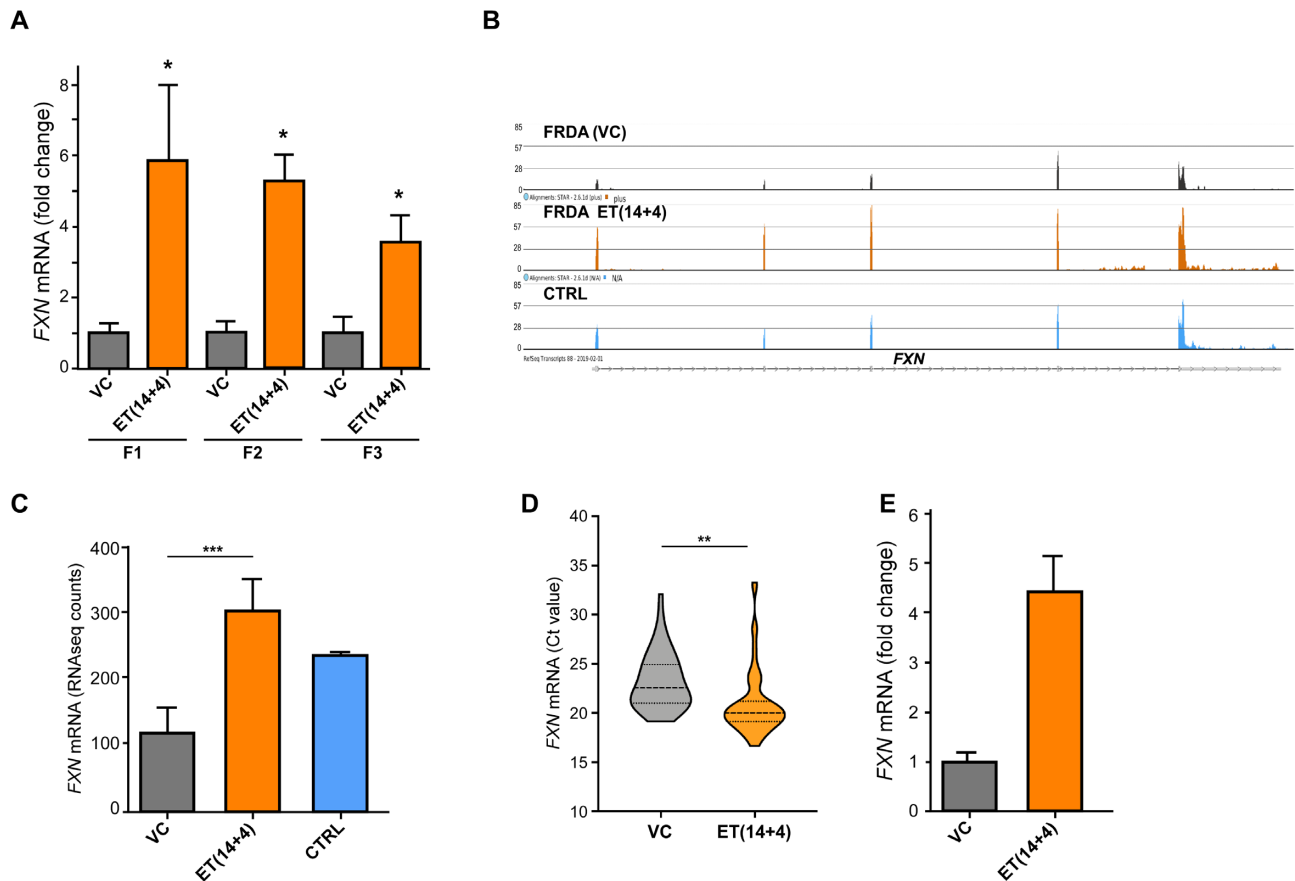


Figure 5. Verification of ET(14 + 4) efficacy using RNA-seq and single-cell qRT-PCR. (A) qRT-PCR analysis of *FXN* mRNA levels in three fibroblast lines derived from different FRDA patients. Data were normalized to *GAPDH* mRNA expression and are shown relative to vehicle control transfection (VC, gray bars). ET(14 + 4) were transfected at 30 nM each. Results are an average of three or more independent experiments. Error bars indicate StDev; * $P < 0.05$. (B) RNA-seq analysis of *FXN* mRNA levels in FRDA fibroblast lines treated with vehicle control (VC, alignment shown in black), ET(14 + 4) (30 nM each; alignment shown in orange) and control unaffected fibroblast cells (CTRL, alignment shown in blue). VC and ET(14 + 4) represent two independent experiments (two treatments and two RNA-seq analyses) and CTRL represents two independent RNA-seq reactions, each using different control fibroblasts (see Supplementary Table S2 for details). (C) Quantitative analysis of the RNA-seq results. *FXN* mRNA expression is represented as normalized RNA-seq counts; *** $P < 0.001$. (D) Results of single-cell qRT-PCR analysis of *FXN* mRNA levels after treatment of FRDA fibroblasts with ET(14 + 4) or vehicle control (VC). Expression of the transcript in Ct values per cell is presented; ** $P < 0.01$. (E) *FXN* mRNA level was determined by standard qRT-PCR in the cells remaining after single-cell Fluidigm C1 sorting; data normalized to *GAPDH* expression. Error bars indicate StDev of three PCR technical replicates.

observed that half-life of the *FXN* mRNA is ~4 h longer in control cells compared to FRDA (vehicle treated), suggesting that the condition of stress induced by low frataxin levels may affect the half-lives of selected mRNAs and thus contribute to the molecular phenotype of the disease. In summary, these results demonstrate that ONs targeting the 5' and 3' ends of the *FXN* mRNA significantly elevate steady-state levels of the mRNA and protein via increased transcript stability. This strategy represents an entirely novel approach to upregulate levels of frataxin in FRDA cells that could also be applicable to other diseases caused by haploinsufficiency of an otherwise intact messenger RNA.

DISCUSSION

Since the discovery of the molecular basis of FRDA, an increase of frataxin levels remains the primary therapeutic goal for this disease. The strategies explored thus far include transcriptional upregulation of the silenced *FXN* lo-

cus via chromatin targeting compounds or interference with noncanonical DNA and/or DNA/RNA structures formed by the expanded GAAs and targeting other pathways that may reduce transcriptional competence of the mutated *FXN* gene. Another group of strategies aimed to increase levels of frataxin includes direct protein supplementation, *FXN* gene delivery via viral vectors, cell therapy and protein stabilization (12,14,15,55). Irrespective of drawbacks and obstacles associated with various experimental therapies, practically all above-mentioned strategies remain viable options for future treatment of FRDA. Hence, it is critical to continue improving these approaches and developing new strategies aimed to alleviate frataxin insufficiency in patient cells.

The premise of this study relies on the fact that all FRDA patients produce *FXN* mRNA, although in significantly lower quantities than unaffected individuals and asymptomatic carriers. This fraction of *FXN* mRNA represents a perfect transcript capable of serving as a template to yield

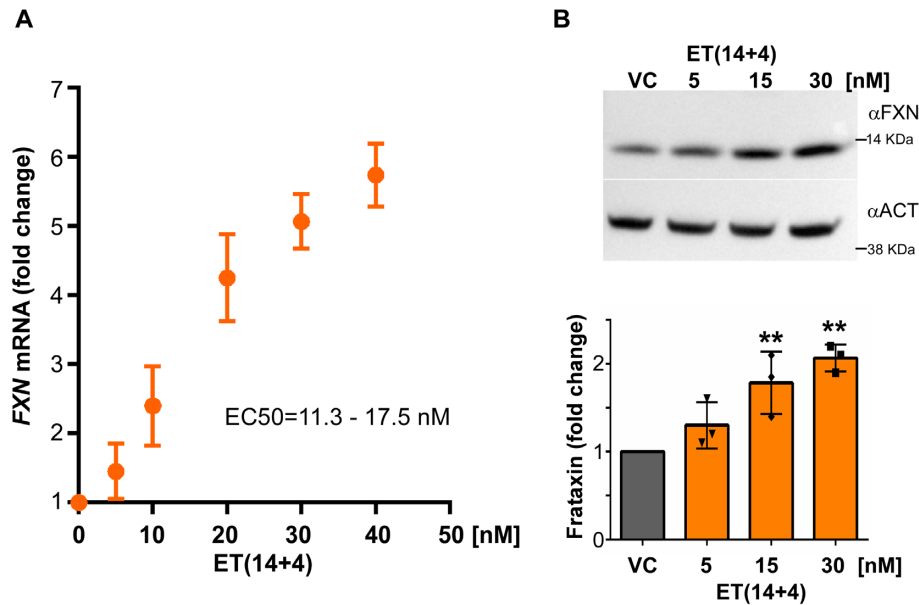


Figure 6. Effect of concentration of ET(14 + 4) on frataxin level. (A) Increase of *FXN* mRNA levels in FRDA fibroblasts transfected with increasing concentrations of ET(14 + 4) in the range of 5–40 nM. Data were collected from three independent experiments ($n = 3$); *FXN* mRNA level was normalized to *GAPDH* mRNA. (B) Increase of frataxin level as a function of ET(14 + 4) concentration (5–30 nM). Actin was used as a loading control and for normalization; data averaged from three independent experiments with error bars indicating StDev; * $P < 0.05$.

functional frataxin protein. Thus, a possible alternative to increasing endogenous transcription or delivering exogenous gene/protein is to develop an approach to allow cells to use the *FXN* mRNA that is already available more efficiently or for a longer time.

In this work, we demonstrated a novel approach to increase intracellular levels of *FXN* mRNA and protein based on targeting of mRNA ends. To minimize the possibility that off-target effects of the ON treatment influence measurements of the *FXN* transcript, we employed three unbiased approaches: absolute qRT-PCR determinations (based on initial mRNA quantitation, not housekeeping normalization), single-cell qRT-PCR with data expressed per individual cell and finally unbiased RNA-seq.

All cellular mRNAs are subjected to continuous turnover. Extending the half-life of mRNA and therefore its availability as a template for translation will result in increased steady-state levels of the encoded protein. RNA decay occurs predominantly via exonucleolytic cleavage of 5' or 3' mRNA ends (56–58). Preventing or slowing down the kinetics of decay processes can increase levels of *FXN* mRNA and ultimately result in upregulation of frataxin levels in FRDA cells. Our research strategy is based on sterically blocking the 5' end of the mRNA as well as the 3' region in the vicinity of the pA signal. A significant increase of the *FXN* mRNA half-life following end-targeting ON treatment strongly indicated that mRNA degradation/turnover is the primary mechanism of action of these ONs. Importantly, in contrast to the approaches targeting transcription proficiency (e.g. histone modifications, noncanonical DNA or DNA/RNA conformations), the chromatin status of the *FXN* locus is unchanged, suggesting that the rate of mRNA production is not changed after end-targeting ON treatment.

We observed a quantitative difference between the effects of the ONs on *FXN* mRNA versus frataxin protein in FRDA cells. While a 4–5-fold increase of the *FXN* transcript was detected in a typical experiment, frataxin levels were elevated to a lesser extent, not exceeding 2–2.5-fold increase over vehicle controls. Prior studies on *FXN* gene reactivation demonstrated similar trends (59). A possibility exists that the global translational apparatus of FRDA cells is impaired and not as efficient as unaffected controls. In support, our prior work demonstrated that expression of numerous ribosomal genes and translation control factors is in fact reduced in FRDA fibroblasts (41). We cannot also rule out the possibility that end-targeting ONs not only influence *FXN* mRNA half-life but simultaneously affect its translation via interference with structures of 5' and/or 3' UTRs. Differential effects of some of the ON pairs [e.g. ET(2 + 3) versus ET(14 + 4)] on frataxin level, despite their comparable effect on *FXN* mRNA, may result from selective inhibitory effects on frataxin translation. Results of our comparative analyses of the effect of individual ONs versus a combination of two ONs on frataxin protein in FRDA cells also suggest that simultaneously targeting 5' and 3' UTRs may impede translation to a greater extent than single ON treatments. It has been demonstrated that binding of ONs to 5' UTRs may decrease the efficiency of translation initiation (38,60). Based on computational modeling [Mfold (61)], both 5' end targeting ONs (ET2 and ET14) interact with *FXN* mRNA at a highly structured region upstream of the translation start site (Supplementary Figure S2), and potentially could cause interference. Future studies using polyribosome profiling and FRDA animal models may help in understanding the effect of ON–transcript interactions on translation and pave the path for developing single or combination ON treatment strategies.

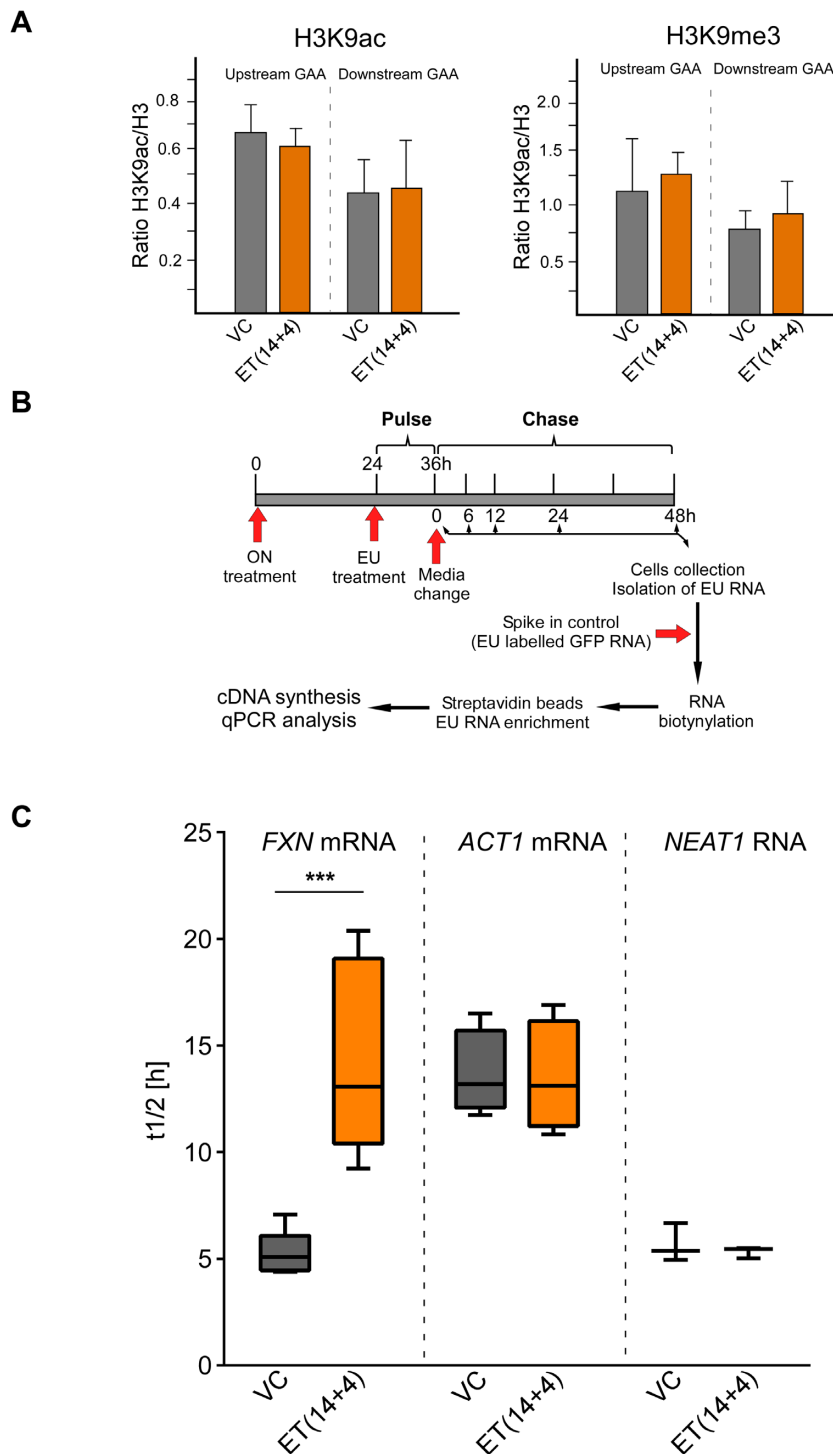


Figure 7. End-targeting ON treatment increases *FXN* mRNA half-life but does not change chromatin status in the vicinity of the GAA repeats. (A) ChIP experiments measuring abundance of histone H3K9ac or H3K9me3 marks upstream and downstream of the GAAs in FRDA fibroblasts transfected with ET(14 + 4) at 30 nM or vehicle control (VC). Signals are normalized to total histone H3. Results of two independent immunoprecipitation experiments are shown. (B) Schematic diagram of the nascent RNA capture approach used to determine half-life of the *FXN* mRNA (see the 'Materials and Methods' section for details). (C) *FXN* mRNA half-life is increased upon treatment of FRDA cells with ET(14 + 4) compared to vehicle-treated cells, while $t_{1/2}$ values of *ACT1* mRNA and *NEAT1* RNA are not affected. Data from three to four independent nascent RNA capture experiments are shown; *** $P < 0.001$.

Interestingly, when the most efficacious ONs were applied to control cells (non-FRDA), an increase of *FXN* mRNA (slightly lower than that in FRDA cells) expression without an accompanying increase of frataxin protein was observed. This effect was confirmed in three different control lines. Steady-state frataxin levels appear to be well controlled as the upregulation of this protein induces toxicity similar to its downregulation (49,50). Thus, upregulation of endogenous frataxin in control cells is likely to initiate a cellular response aimed to mitigate toxic effects of frataxin upregulation. This is not the case in FRDA cells that demonstrate low basal levels of frataxin.

The exact mechanism of how end-targeting ONs can affect mRNA half-life is not understood, though we can speculate that hindering interaction/activity of mRNA degradation complexes likely contributes. A plausible alternative, at least for ONs targeting the 3' UTR, would be interference with miRNAs regulating the *FXN* transcript. However, analysis of our comprehensive miRNA-seq data from FRDA and control fibroblasts (45) indicates that none of the miRNAs expressed in fibroblasts is likely to compete with ET3 or ET4 for binding of the *FXN* transcript 3' UTR. Further studies designed to dissect mechanism(s) responsible for extension of the mRNA half-life may result in development of more efficient strategies. Furthermore, advancing studies aimed to define tissue or cell-specific diversity of the 5' and 3' mRNA ends will be necessary to determine broad applicability of therapeutic strategies targeting these noncoding regions.

Although initially antisense ONs were mainly designed to eradicate transcripts, recent studies have demonstrated their versatility. In fact, ONs can decrease or increase levels of their mRNA targets, affecting translation directly and inducing changes in maturation of pre-mRNA via exon skipping or inclusion, or indirectly by affecting expression via alleviation of R-loop formation (29,32–34,62,63). More recently, selected ONs targeting pre-mRNA were shown to affect transcription kinetics (64). Thus, it appears that nearly all processes occurring at the DNA/RNA level can be modulated by appropriately designed antisense ONs (62,63).

Presently, 10 ON-based drugs have been approved by the US Food and Drug Administration and/or European Medicines Agency, and ~30 additional therapeutics are being evaluated in clinical trials (63). None of the ~40 repeat expansion diseases has been successfully targeted for treatment by ONs; however, many clinical trials targeting Huntington's disease and C9ORF72 amyotrophic lateral sclerosis are ongoing or have been recently completed (63). No therapy or cure exists for FRDA and targeting the frataxin deficit remains one of the most important goals. Evaluating efficacy of ON-based approaches, either stimulating transcription or stabilizing existing transcripts, in animal models presents the next step in the development of successful leads for clinical development.

DATA AVAILABILITY

RNA-seq data files from FRDA and control fibroblasts are available at GEO accession GSE104288 and upon request.

SUPPLEMENTARY DATA

Supplementary Data are available at NAR Online.

ACKNOWLEDGEMENTS

We thank MaxCyte for providing the MaxCyte STX system and related supplies. D.R.C. is the Rusty Kelley Professor of Biomedical Science. The research was also supported by a generous gift from the Doremus family.

FUNDING

National Institutes of Health [R01NS081366 to M.N., R35GM118103 to D.R.C.]; Muscular Dystrophy Association [MDA418838 to M.N.]; Friedreich's Ataxia Research Alliance [to M.N. and D.R.C.]; Welch Foundation [I-1244 to D.R.C.]; University of Texas Southwestern Medical Center [Paul D. Wellstone MDCRC Trainee Fellowship Award to X.S.]. Funding for open access charge: National Institutes of Health [R01NS081366].

Conflict of interest statement. C.W., D.P. and B.B. are employees of Translate Bio; at the time of data generation, J.J.C. was an employee of Translate Bio. Translate Bio sponsored in part work conducted in this study; however, it had no influence on the experimental procedures, data acquisition and analyses. Critical experiments were conducted independently and blindly in three laboratories.

REFERENCES

- Pandolfo, M. (2006) Friedreich's ataxia. In: Wells, R.D. and Ashizawa, T. (eds). *Genetic Instabilities and Neurological Diseases*, 2nd edn. Elsevier–Academic Press, San Diego, CA, pp. 277–296.
- Campuzano, V., Montermini, L., Molto, M.D., Pianese, L., Cossee, M., Cavalcanti, F., Monros, E., Rodius, F., Duclos, F., Monticelli, A. *et al.* (1996) Friedreich's ataxia: autosomal recessive disease caused by an intronic GAA triplet repeat expansion. *Science*, **271**, 1423–1427.
- Pandolfo, M. (2009) Friedreich ataxia: the clinical picture. *J. Neurol.*, **256**, 3–8.
- Marmolino, D. (2011) Friedreich's ataxia: past, present and future. *Brain Res. Rev.*, **67**, 311–330.
- Cossee, M., Durr, A., Schmitt, M., Dahl, N., Trouillas, P., Allinson, P., Kostrzewa, M., Nivelon-Chevallier, A., Gustavson, K.H., Kohlschütter, A. *et al.* (1999) Friedreich's ataxia: point mutations and clinical presentation of compound heterozygotes. *Ann. Neurol.*, **45**, 200–206.
- Colin, F., Martelli, A., Clemancey, M., Latour, J.M., Gambarelli, S., Zeppieri, L., Birck, C., Page, A., Puccio, H. and Ollagnier de Choudens, S. (2013) Mammalian frataxin controls sulfur production and iron entry during *de novo* Fe₄S₄ cluster assembly. *J. Am. Chem. Soc.*, **135**, 733–740.
- Pastore, A. and Puccio, H. (2013) Frataxin: a protein in search for a function. *J. Neurochem.*, **126**, 43–52.
- Pianese, L., Turano, M., Lo Casale, M.S., De Biase, I., Giacchetti, M., Monticelli, A., Criscuolo, C., Filla, A. and Coccozza, S. (2004) Real time PCR quantification of frataxin mRNA in the peripheral blood leucocytes of Friedreich ataxia patients and carriers. *J. Neurol. Neurosurg. Psychiatry*, **75**, 1061–1063.
- Li, Y., Lu, Y., Polak, U., Lin, K., Shen, J., Farmer, J., Seyer, L., Bhalla, A.D., Rozwadowska, N., Lynch, D.R. *et al.* (2015) Expanded GAA repeats impede transcription elongation through the FXN gene and induce transcriptional silencing that is restricted to the FXN locus. *Hum. Mol. Genet.*, **24**, 6932–6943.
- Zhang, S., Napierala, M. and Napierala, J.S. (2019) Therapeutic prospects for Friedreich's ataxia. *Trends Pharmacol. Sci.*, **40**, 229–233.
- Gottesfeld, J.M. (2019) Molecular mechanisms and therapeutics for the GAA.TTC expansion disease Friedreich ataxia. *Neurotherapeutics*, **4**, 1032–1049.

12. Perdomini, M., Belbellaa, B., Monassier, L., Reutenauer, L., Messaddeq, N., Cartier, N., Crystal, R.G., Aubourg, P. and Puccio, H. (2014) Prevention and reversal of severe mitochondrial cardiomyopathy by gene therapy in a mouse model of Friedreich's ataxia. *Nat. Med.*, **20**, 542–547.
13. Alfedi, G., Luffarelli, R., Condo, I., Pedini, G., Mannucci, L., Massaro, D.S., Benini, M., Toschi, N., Alaimo, G., Panarello, L. *et al.* (2019) Drug repositioning screening identifies etravirine as a potential therapeutic for Friedreich's ataxia. *Mov. Disord.*, **34**, 323–334.
14. Vyas, P.M., Tomamichel, W.J., Pride, P.M., Babbey, C.M., Wang, Q., Mercier, J., Martin, E.M. and Payne, R.M. (2012) A TAT-frataxin fusion protein increases lifespan and cardiac function in a conditional Friedreich's ataxia mouse model. *Hum. Mol. Genet.*, **21**, 1230–1247.
15. Rocca, C.J., Goodman, S.M., Dulin, J.N., Haquang, J.H., Gertsman, I., Blondelle, J., Smith, J.L.M., Heyser, C.J. and Cherqui, S. (2017) Transplantation of wild-type mouse hematopoietic stem and progenitor cells ameliorates deficits in a mouse model of Friedreich's ataxia. *Sci. Transl. Med.*, **9**, eaaj2347.
16. Zesiewicz, T.A., Hancock, J., Ghanekar, S.D., Kuo, S.H., Dohse, C.A. and Vega, J. (2020) Emerging therapies in Friedreich's ataxia. *Exp. Rev. Neurother.*, **20**, 1215–1228.
17. Soragni, E., Miao, W., Iudicello, M., Jacoby, D., De Mercanti, S., Clerico, M., Longo, F., Piga, A., Ku, S., Campau, E. *et al.* (2014) Epigenetic therapy for Friedreich ataxia. *Ann. Neurol.*, **76**, 489–508.
18. Burnett, R., Melander, C., Puckett, J.W., Son, L.S., Wells, R.D., Dervan, P.B. and Gottesfeld, J.M. (2006) DNA sequence-specific polyamides alleviate transcription inhibition associated with long GAA.TTC repeats in Friedreich's ataxia. *Proc. Natl Acad. Sci. U.S.A.*, **103**, 11497–11502.
19. Sakamoto, N., Chastain, P.D., Parniewski, P., Ohshima, K., Pandolfo, M., Griffith, J.D. and Wells, R.D. (1999) Sticky DNA: self-association properties of long GAA.TTC repeats in R.R.Y triplex structures from Friedreich's ataxia. *Mol. Cell*, **3**, 465–475.
20. Groh, M., Lufino, M.M., Wade-Martins, R. and Gromak, N. (2014) R-loops associated with triplet repeat expansions promote gene silencing in Friedreich ataxia and fragile X syndrome. *PLoS Genet.*, **10**, e1004318.
21. Butler, J.S. and Napierala, M. (2015) Friedreich's ataxia—a case of aberrant transcription termination? *Transcription*, **6**, 33–36.
22. Rai, M., Soragni, E., Jenssen, K., Burnett, R., Herman, D., Coppola, G., Geschwind, D.H., Gottesfeld, J.M. and Pandolfo, M. (2008) HDAC inhibitors correct frataxin deficiency in a Friedreich ataxia mouse model. *PLoS One*, **3**, e1958.
23. Herman, D., Jenssen, K., Burnett, R., Soragni, E., Perlman, S.L. and Gottesfeld, J.M. (2006) Histone deacetylase inhibitors reverse gene silencing in Friedreich's ataxia. *Nat. Chem. Biol.*, **2**, 551–558.
24. Erwin, G.S., Grieshop, M.P., Ali, A., Qi, J., Lawlor, M., Kumar, D., Ahmad, I., McNally, A., Teider, N., Worringer, K. *et al.* (2017) Synthetic transcription elongation factors license transcription across repressive chromatin. *Science*, **358**, 1617–1622.
25. Vilema-Enriquez, G., Quinlan, R., Kilfeather, P., Mazzone, R., Saqlain, S., Del Molino Del Barrio, I., Donato, A., Corda, G., Li, F., Vedadi, M. *et al.* (2020) Inhibition of the SUV4-20 H1 histone methyltransferase increases frataxin expression in Friedreich's ataxia patient cells. *J. Biol. Chem.*, **295**, 17973–17985.
26. Shen, X., Wong, J., Prakash, T.P., Rigo, F., Li, Y., Napierala, M. and Corey, D.R. (2020) Progress towards drug discovery for Friedreich's ataxia: identifying synthetic oligonucleotides that more potently activate expression of human frataxin protein. *Bioorg. Med. Chem.*, **28**, 115472.
27. Shen, X., Beasley, S., Putman, J.N., Li, Y., Prakash, T.P., Rigo, F., Napierala, M. and Corey, D.R. (2019) Efficient electroporation of neuronal cells using synthetic oligonucleotides: identifying duplex RNA and antisense oligonucleotide activators of human frataxin expression. *RNA*, **25**, 1118–1129.
28. Shen, X., Kilikevicius, A., O'Reilly, D., Prakash, T.P., Damha, M.J., Rigo, F. and Corey, D.R. (2018) Activating frataxin expression by single-stranded siRNAs targeting the GAA repeat expansion. *Bioorg. Med. Chem. Lett.*, **28**, 2850–2855.
29. Li, L., Matsui, M. and Corey, D.R. (2016) Activating frataxin expression by repeat-targeted nucleic acids. *Nat. Commun.*, **7**, 10606.
30. Bergquist, H., Rocha, C.S., Alvarez-Ascencio, R., Nguyen, C.H., Rutland, M.W., Smith, C.I., Good, L., Nielsen, P.E. and Zain, R. (2016) Disruption of higher order DNA structures in Friedreich's ataxia (GAA)_n repeats by PNA or LNA targeting. *PLoS One*, **11**, e0165788.
31. Grabczyk, E. and Usdin, K. (2000) Alleviating transcript insufficiency caused by Friedreich's ataxia triplet repeats. *Nucleic Acids Res.*, **28**, 4930–4937.
32. Magen, I. and Hornstein, E. (2014) Oligonucleotide-based therapy for neurodegenerative diseases. *Brain Res.*, **1584**, 116–128.
33. Evers, M.M., Toonen, L.J. and van Roon-Mom, W.M. (2015) Antisense oligonucleotides in therapy for neurodegenerative disorders. *Adv. Drug Deliv. Rev.*, **87**, 90–103.
34. Lee, J.J. and Yokota, T. (2013) Antisense therapy in neurology. *J. Pers. Med.*, **3**, 144–176.
35. Matsui, M., Sakurai, F., Elbashir, S., Foster, D.J., Manoharan, M. and Corey, D.R. (2010) Activation of LDL receptor expression by small RNAs complementary to a noncoding transcript that overlaps the LDLR promoter. *Chem. Biol.*, **17**, 1344–1355.
36. Lim, K.H., Han, Z., Jeon, H.Y., Kach, J., Jing, E., Weyn-Vanhenyryck, S., Downs, M., Corriero, A., Oh, R., Scharner, J. *et al.* (2020) Antisense oligonucleotide modulation of non-productive alternative splicing upregulates gene expression. *Nat. Commun.*, **11**, 3501.
37. Liang, X.H., Shen, W., Sun, H., Migawa, M.T., Vickers, T.A. and Crooke, S.T. (2016) Translation efficiency of mRNAs is increased by antisense oligonucleotides targeting upstream open reading frames. *Nat. Biotechnol.*, **34**, 875–880.
38. Liang, X.H., Sun, H., Shen, W., Wang, S., Yao, J., Migawa, M.T., Bui, H.H., Damle, S.S., Riney, S., Graham, M.J. *et al.* (2017) Antisense oligonucleotides targeting translation inhibitory elements in 5' UTRs can selectively increase protein levels. *Nucleic Acids Res.*, **45**, 9528–9546.
39. Li, L., Shen, X., Liu, Z., Norrbom, M., Prakash, T.P., O'Reilly, D., Sharma, V.K., Damha, M.J., Watts, J.K., Rigo, F. *et al.* (2018) Activation of frataxin protein expression by antisense oligonucleotides targeting the mutant expanded repeat. *Nucleic Acid Ther.*, **28**, 23–33.
40. Li, Y., Polak, U., Clark, A.D., Bhalla, A.D., Chen, Y.Y., Li, J., Farmer, J., Seyer, L., Lynch, D., Butler, J.S. *et al.* (2016) Establishment and maintenance of primary fibroblast repositories for rare diseases—Friedreich's ataxia example. *Biopreserv. Biobank.*, **14**, 324–329.
41. Napierala, J.S., Li, Y., Lu, Y., Lin, K., Hauser, L.A., Lynch, D.R. and Napierala, M. (2017) Comprehensive analysis of gene expression patterns in Friedreich's ataxia fibroblasts by RNA sequencing reveals altered levels of protein synthesis factors and solute carriers. *Dis. Models Mech.*, **10**, 1353–1369.
42. Li, J., Rozwadowska, N., Clark, A., Fil, D., Napierala, J.S. and Napierala, M. (2019) Excision of the expanded GAA repeats corrects cardiomyopathy phenotypes of iPSC-derived Friedreich's ataxia cardiomyocytes. *Stem Cell Res.*, **40**, 101529.
43. Polak, U., Li, Y., Butler, J.S. and Napierala, M. (2016) Alleviating GAA repeat induced transcriptional silencing of the Friedreich's ataxia gene during somatic cell reprogramming. *Stem Cells Dev.*, **25**, 1788–1800.
44. Li, Y., Polak, U., Bhalla, A.D., Rozwadowska, N., Butler, J.S., Lynch, D.R., Dent, S.Y. and Napierala, M. (2015) Excision of expanded GAA repeats alleviates the molecular phenotype of Friedreich's ataxia. *Mol. Ther.*, **23**, 1055–1065.
45. Misiolek, J.O., Schreiber, A.M., Urbanek-Trzeciak, M.O., Jazurek-Ciesiolka, M., Hauser, L.A., Lynch, D.R., Napierala, J.S. and Napierala, M. (2020) A comprehensive transcriptome analysis identifies FXN and BDNF as novel targets of miRNAs in Friedreich's ataxia patients. *Mol. Neurobiol.*, **57**, 2639–2653.
46. Chen, C.Y., Ezzeddine, N. and Shyu, A.B. (2008) Messenger RNA half-life measurements in mammalian cells. *Methods Enzymol.*, **448**, 335–357.
47. Bhagavati, S. (2016) Doubts about therapy for neurological diseases with antisense oligonucleotides. *JAMA Neurol.*, **73**, 1502.
48. Rodden, L.N., Chutake, Y.K., Gilliam, K., Lam, C., Soragni, E., Hauser, L., Gilliam, M., Wiley, G., Anderson, M.P., Gottesfeld, J.M. *et al.* (2021) Methylated and unmethylated epialleles support variegated epigenetic silencing in Friedreich ataxia. *Hum. Mol. Genet.*, **29**, 3818–3829.
49. Vannocci, T., Notario Manzano, R., Beccalli, O., Bettegazzi, B., Grohovaz, F., Cinque, G., de Riso, A., Quaroni, L., Codazzi, F. and Pastore, A. (2018) Adding a temporal dimension to the study of

- Friedreich's ataxia: the effect of frataxin overexpression in a human cell model. *Dis. Models Mech.*, **11**, dmm032706.
50. Belbellaa,B., Reutenauer,L., Messaddeq,N., Monassier,L. and Puccio,H. (2020) High levels of frataxin overexpression lead to mitochondrial and cardiac toxicity in mouse models. *Mol. Ther. Methods Clin. Dev.*, **19**, 120–138.
51. Al-Mahdawi,S., Pinto,R.M., Ismail,O., Varshney,D., Lympéri,S., Sandi,C., Trabzuni,D. and Pook,M. (2008) The Friedreich ataxia GAA repeat expansion mutation induces comparable epigenetic changes in human and transgenic mouse brain and heart tissues. *Hum. Mol. Genet.*, **17**, 735–746.
52. Tani,H. and Akimitsu,N. (2012) Genome-wide technology for determining RNA stability in mammalian cells: historical perspective and recent advantages based on modified nucleotide labeling. *RNA Biol.*, **9**, 1233–1238.
53. Jao,C.Y. and Salic,A. (2008) Exploring RNA transcription and turnover *in vivo* by using click chemistry. *Proc. Natl Acad. Sci. U.S.A.*, **105**, 15779–15784.
54. Duan,J., Shi,J., Ge,X., Dolken,L., Moy,W., He,D., Shi,S., Sanders,A.R., Ross,J. and Gejman,P.V. (2013) Genome-wide survey of interindividual differences of RNA stability in human lymphoblastoid cell lines. *Sci. Rep.*, **3**, 1318.
55. Rufini,A., Fortuni,S., Arcuri,G., Condo,I., Serio,D., Incani,O., Malisan,F., Ventura,N. and Testi,R. (2011) Preventing the ubiquitin-proteasome-dependent degradation of frataxin, the protein defective in Friedreich's ataxia. *Hum. Mol. Genet.*, **20**, 1253–1261.
56. Schoenberg,D.R. and Maquat,L.E. (2012) Regulation of cytoplasmic mRNA decay. *Nat. Rev. Genet.*, **13**, 246–259.
57. Chen,C.Y. and Shyu,A.B. (2011) Mechanisms of deadenylation-dependent decay. *Wiley Interdiscip. Rev. RNA*, **2**, 167–183.
58. Song,M.G., Li,Y. and Kiledjian,M. (2010) Multiple mRNA decapping enzymes in mammalian cells. *Mol. Cell*, **40**, 423–432.
59. Georges,P., Boza-Moran,M.G., Gide,J., Peche,G.A., Foret,B., Bayot,A., Rustin,P., Peschanski,M., Martinat,C. and Aubry,L. (2019) Induced pluripotent stem cells-derived neurons from patients with Friedreich ataxia exhibit differential sensitivity to resveratrol and nicotinamide. *Sci. Rep.*, **9**, 14568.
60. Johansson,H.E., Belsham,G.J., Sproat,B.S. and Hentze,M.W. (1994) Target-specific arrest of mRNA translation by antisense 2'-O-alkyloligoribonucleotides. *Nucleic Acids Res.*, **22**, 4591–4598.
61. Zuker,M. (2003) Mfold web server for nucleic acid folding and hybridization prediction. *Nucleic Acids Res.*, **31**, 3406–3415.
62. Crooke,S.T., Witztum,J.L., Bennett,C.F. and Baker,B.F. (2018) RNA-targeted therapeutics. *Cell Metab.*, **27**, 714–739.
63. Roberts,T.C., Langer,R. and Wood,M.J.A. (2020) Advances in oligonucleotide drug delivery. *Nat. Rev. Drug Discov.*, **19**, 673–694.
64. Lai,F., Damle,S.S., Ling,K.K. and Rigo,F. (2020) Directed RNase H cleavage of nascent transcripts causes transcription termination. *Mol. Cell*, **77**, 1032–1043.